Fiber-integrated 780 nm source for visible parametric generation

D. J. J. Hu,[1,2,5,*] R. T. Murray,[1,5] T. Legg,[3] T. H. Runcorn,[1] M. Zhang,[1] R. I. Woodward,[1] J. L. Lim,[2,4] Y. Wang,[2] F. Luan,[4] B. Gu,[4] P. P. Shum,[4] E. J. R. Kelleher,[1] S. V. Popov,[1] and J. R. Taylor[1]

[1]*Femtosecond Optics Group, Department of Physics, Imperial College London, Prince Consort Road, London SW7 2BW, UK*

[2]*RF, Antenna and Optical Department, Institute for Infocomm Research, Agency for Science, Technology and Research, Singapore*

[3]*Gooch and Housego, Broomhill Way, Torquay TQ2 7QL, UK*

[4]*School of Electrical and Electronic Engineering, Nanyang Technological University, Singapore*

[5]*Both authors contributed equally to this work.*

[*]*jjhu@i2r.a-star.edu.sg*

Abstract: We report the development of a fully fiber-integrated pulsed master oscillator power fibre amplifier (MOPFA) source at 780 nm, producing 3.5 W of average power with 410 ps pulses at a repetition rate of 50 MHz. The source consists of an intensity modulated 1560 nm laser diode amplified in an erbium fiber amplifier chain, followed by a fiber coupled periodically poled lithium niobate crystal module for frequency doubling. The source is then used for generating visible light through four-wave mixing in a length of highly nonlinear photonic crystal fiber: 105 mW at 668 nm and 95 mW at 662 nm are obtained, with pump to anti-Stokes conversion slope efficiencies exceeding 6% in both cases.

OCIS codes: (190.4370) Nonlinear optics, fibers; (190.4382) Four-wave mixing.

References and links

1. P. A. Franken, A. E. Hill, C. W. Peters, and G. Weinreich, "Generation of optical harmonics," Phys. Rev. Lett. **7**(4), 118-119 (1961).
2. S. V. Popov, S. V. Chernikov, and J. R. Taylor, "6W average power green light generation using seeded high power Yb amplifier and periodically poled KTP," Opt. Comm. **174**(1-4), 231-234 (2000).
3. S. W. Chiow, T. Kovachy, J. M. Hogan, and M. A. Kasevish, "Generation of 43 W of quasi-continuous 780 nm laser light via high-efficiency, single-pass frequency doubling in periodically poled lithium niobate crystals," Opt. Lett. **37**(18), 3861-3863 (2012).
4. M. Laroche, C. Bartolacci, B. Cadier, H. Gilles, S. Girard, L. Lablonde, and T. Robin, "Generation of 520 mW pulsed blue light by frequency doubling of an all-fiberized 978 nm Yb-doped fiber laser source," Opt. Lett. **36**(19), 3909-3911 (2011).
5. E. M. Dianov, "Bismuth-doped optical fibers: a challenging active medium for near-IR lasers and optical amplifiers," Light Sci. Appl. **1**(5), e12 (2012).
6. B. H. Chapman, E. J. R. Kelleher, S. V. Popov, K. M. Golant, J. Puustinen, O. Okhotnikov, and J. R. Taylor, "Picosecond bismuth-doped fiber MOPFA for frequency conversion," Opt. Lett. **36**(19), 3792-3794 (2011).
7. J. D. Harvey, R. Leonhardt, S. Coen, G. K. L. Wong, J. C. Knight, W. J. Wadsworth and P. St. J. Russell, "Scalar modulation instability in the normal dispersion regime by use of a photonic crystal fiber," Opt. Lett. **28**(22), 2225-2227 (2003).
8. A. Y. H. Chen, G. K. L. Wong, S. G. Murdoch, R. Leonhardt, J. D. Harvey, J. C. Knight, W. J. Wadsworth, and P. St. J. Russell, "Widely tunable optical parametric generation in a photonic crystal fiber," Opt. Lett. **30**(7), 762-764 (2005).
9. L. Lavoute, J. C. Knight, P. Dupriez, and W. J. Wadsworth, "High power red and near-IR generation using four wave mixing in all integrated fiber laser systems," Opt. Express **18**(15), 16193-16205 (2010).
10. A. Herzog, A. Shamir, and A. A. Ishaaya, "Wavelength conversion of nanosecond pulses to the mid-IR in photonic crystal fibers," Opt. Lett. **37**(1), 82-84 (2012).
11. S. W. Hell and J. Wichmann, "Breaking the diffraction resolution limit by stimulated emission: stimulated-emission-depletion fluorescence microscopy," Opt. Lett. **19**(11), 780-782 (1994).

#223363 - $15.00 USD Received 17 Sep 2014; revised 21 Oct 2014; accepted 21 Oct 2014; published 20 Nov 2014

12. D. Wildanger, E. Rittweger, L. Kastrup and S. W. Hell, "STED microscopy with a supercontinuum laser source," Opt. Express 16(13), 9614-9621 (2008).

1. Introduction

Frequency doubling is a commonly used method of nonlinear frequency conversion, capable of converting radiation from well-established lasing transitions to other areas of the spectrum [1]. In particular, the doubling of master oscillator power fiber amplifier (MOPFA) systems, based on common rare earth dopants such as ytterbium or erbium, to generate visible and near-infrared (NIR) light is a powerful technique [2-4]. However, the generation of red light through frequency doubling of MOPFA systems is more difficult, owing to the lack of well-developed high power fiber based systems operating in the 1.2.-1.3 μm regime (bismuth-doped fiber is an emerging technology in this region, but not yet commercially available [5,6]). One way to extend the spectral reach of a frequency doubled MOPFA laser system is through further χ^3 based nonlinear interactions. Four-wave mixing (FWM) is an attractive option, where by pumping in the low normal dispersion region of a suitably designed optical fiber it is possible to generate parametric sidebands widely spaced from the pump wavelength [7-10]. In this way, it is possible to create fully fiberized sources of radiation at target wavelengths throughout the visible region of the spectrum.

In this letter, we present a high-power fully fiberized frequency doubled pulsed source; the system herein produces 3.5 W average power at 780 nm, but the module has generated up to 5 W. We then pump a length of highly nonlinear photonic crystal fiber (PCF) to further shift into the red region of the spectrum and generate ≥ 95 mW of light at 662 and 668 nm through degenerate-pump FWM. Corresponding Stokes sidebands in the NIR around 940 nm are observed. Such a source producing synchronized pairs of pulses in the 200-400 ps range could prove useful for STED microscopy applications, where spatially and temporally overlapping pairs of visible/near-visible pulses are needed [11,12].

2. Experiment and discussion

The schematic of the MOPFA system, the frequency doubling module and the parametric wavelength conversion stage are shown in Fig. 1. The seed laser consisted of a distributed feedback laser diode (Nortel Networks LC25W*BA) centered around 1560 nm, a commercial erbium doped fiber amplifier (EDFA1), a fiber polarization controller (PC), and a fiber pigtailed polarization-maintaining (PM) Mach-Zehnder amplitude modulator (MZAM) (Sumitomo 10GHz TMXH-1). A DC bias voltage was applied across the MZAM to control the extinction of the device. A tunable electrical pulse generator (Geozondas-GZH1132VN) was then used to modulate the MZAM and produce a train of optical pulses. The repetition rate of the pulse generator was set to 50 MHz – lower values of repetition rates (down to 10 MHz) were possible, but 50 MHz was found to produce the highest conversion efficiencies in the frequency conversion module. This was due to nonlinear spectral broadening in the amplifier stages at lower repetition rates, i.e. higher peak powers. The PC was used to adjust the polarization state of the CW laser and maximize the extinction ratio of MZAM.

The amplifier stage consisted of four EDFAs, a tap coupler (2/98) and a fiber PC. The MOPFA produced average output powers up to 15.6 W. The optical spectrum of the amplified pulses from the MOPFA system is plotted in Fig. 2(a). The 3 dB spectral linewidth was measured to be 0.01 nm or less. This measurement was limited by the resolution of the optical spectrum analyzer (OSA). The pulse trace at the monitor port is plotted in Fig. 2(b). The pulses of the monitor port of the tap coupler exhibited pulse full-width at half maximum (FWHM) duration of 430 ps, measured on a 50 GHz sampling oscilloscope with a 20 GHz photodetector. The pump pulse duration could be tuned by adjusting the duration of the electrical pulses driving the MZAM (>300 ps). However, the optimum pump pulse duration was determined by maximizing the anti-Stokes output power in the FWM process, described later. Therefore, all the results presented hereafter were based on a pump system with the following parameters: 50 MHz repetition rate, 430 ps pump pulse duration (measured at the monitor port).

#223363 - $15.00 USD Received 17 Sep 2014; revised 21 Oct 2014; accepted 21 Oct 2014; published 20 Nov 2014

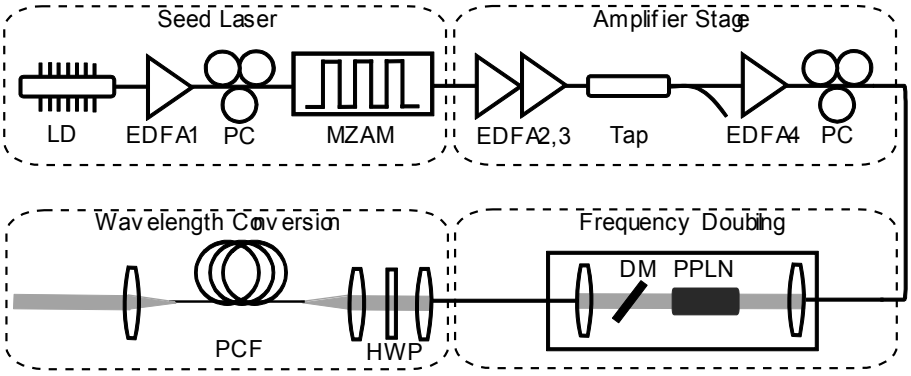

Fig. 1. Experimental setup of the all-fiber 780 nm source by frequency doubling a 1560 nm MOPFA source in a fiber integrated PPLN module, and red parametric generation through four-wave mixing in a highly nonlinear PCF. (LD: laser diode, EDFA (1-4): Erbium doped fiber amplifier, PC: polarization controller, MZAM: Mach-Zehnder amplitude modulator, Tap: optical tap coupler, 2% port is used for monitoring the 1560 nm pulses, PPLN: periodically poled lithium niobate, DM: dichroic mirror, HWP: half waveplate, PCF: a highly nonlinear photonic crystal fiber).

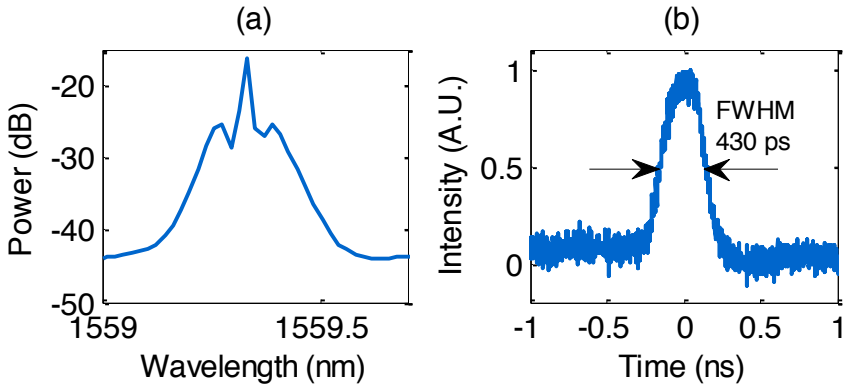

Fig. 2. (a) Spectrum of the amplified 1560 nm pulses after EDFA 4, (b) temporal profile of the 1560 nm pulses of the 2% port of the tap coupler.

The high power 1560 nm MOPFA source was frequency doubled in a fiber-pigtailed periodically poled lithium niobate (PPLN) crystal module developed by Gooch & Housego. The module had peltier thermoelectric cooler (TEC) temperature stabilization of both the crystal housing for efficient second harmonic generation (SHG) and the baseplate to which the optics were mounted to ensure stable fiber coupling. The crystal used in the module was 5 mol% MgO doped congruent lithium niobate with dimensions: 35 mm in length, 3 mm in width and 1 mm in height. The PPLN poling period was 19.48 µm and the SHG was optimum at 70.25 °C. The phase-matching bandwidth of the crystal was 0.35 nm at 1560 nm . The crystal incidence/exit surfaces were AR coated at 1560 nm (R<0.3%)/780 nm (R<0.5%). The output PM fiber (Nufern PM780-HP) was aligned for propagation along the slow axis and maintained the linear polarization state of the 780 nm pulses so a polarization extinction ratio of 15 dB was achieved at the output fiber of the crystal module.

The measured optical spectrum of the frequency doubled 780 nm pulsed laser is shown in Fig. 3(a). The 3 dB linewidth was 0.1 nm or less, this measurement was resolution limited by the OSA. The SHG wavelength was measured to be slightly more than half the fundamental wavelength. However, this was due to a slight miscalibration in the OSA's used to take each spectrum, and was not due to any physical effect. The variation of the SHG

#223363 - $15.00 USD Received 17 Sep 2014; revised 21 Oct 2014; accepted 21 Oct 2014; published 20 Nov 2014

output power with crystal temperature is shown in Fig. 3(b). The measurement was taken with maximum fundamental input power of 15.6 W. The temperature of the crystal's baseplate was kept at 30 °C throughout the experiment. The polarization states of the PCs were kept unchanged during the measurement. A maximum power of 3.5 W of the 780 nm signal was achieved when the crystal temperature was 70.25 °C from which the SHG power rapidly reduced, i.e. the temperature tuning range was about 1.7 °C for the SHG power to drop to half of the peak power. Figure 3(c) illustrates the converted power (solid line) and conversion efficiency (solid line with circles) from fundamental 1560 nm pulses to SHG 780 nm pulses. The PC at the input of the module was used to adjust the polarization state of the amplified 1560 nm pulses in order to maximize the SHG conversion efficiency. For an input power of 15.6 W of 1560 nm fundamental light, 3.5 W of 780 nm light was produced, corresponding to a conversion efficiency of 22.4%. It should be noted that the power amplifier stages used in the MOPFA system, EDFA3 and EDFA4, were non-PM. The system could be made more robust and stable against environmental perturbations by using PM power amplifiers.

The 780 nm temporal pulse profile was characterized using a streak camera (Hamamatsu-OOS-001) and it had duration of 410 ps as shown in Fig. 3(d). The leading edge noticeable on the streak camera trace is due to CW breakthrough in the MZAM. The corresponding pulse peak power was 171 W.

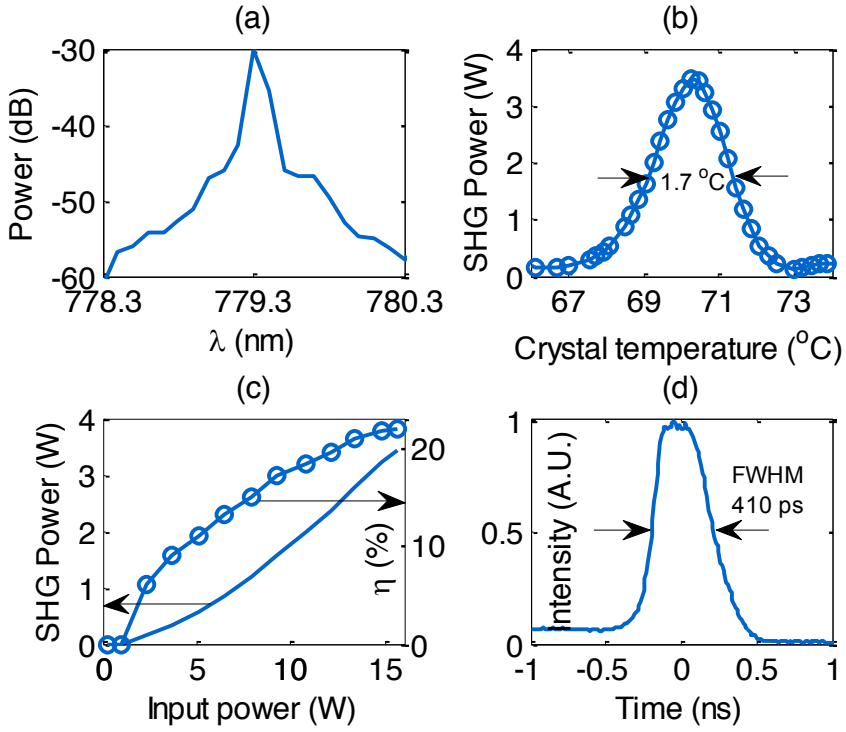

Fig. 3. (a) Spectrum of the frequency doubled output at 780 nm, (b) temperature tuning of the PPLN crystal taken at 15.6 W input power, (c) SHG output power and conversion efficiency at 780 nm as a function of input power at 1560 nm, (d) SHG pulse duration measured on streak camera.

The 780 nm source was then used for FWM experiments detailed in the following paragraphs. We employed a highly nonlinear PCF (Blaze Photonics) and used it to demonstrate scalar degenerate-pump FWM in which the pump, Stokes and anti-Stokes photons lie in the same polarization axes. The scanning electron microscope (SEM) image of

#223363 - $15.00 USD Received 17 Sep 2014; revised 21 Oct 2014; accepted 21 Oct 2014; published 20 Nov 2014

the cross-sectional fiber structure used in this experiment is presented in Fig. 4(a). The core diameter was 2.3 μm, the hole-to-hole distance was 2.6 μm with an air-filling fraction in the holey region of more than 90%. The fiber loss and calculated nonlinear coefficient were 0.089 dB/m and 80 $W^{-1}km^{-1}$ at 790 nm respectively. Due to the slight asymmetry of the hexagon lattice structure and core geometry, the fundamental modes of the PCF were non-degenerate, the calculated group birefringence was 3.0×10^{-5} at 790 nm (RSOFT FEMSIM). Figure 4(b) shows the calculated dispersion profile for both axes. The inset figure shows that the zero-dispersion wavelengths were 786.5 nm and 787.6 nm for the fast and slow axis respectively.

The phasematching condition for degenerate-pump FWM is given by $\Delta\kappa = 2\beta(p) - \beta(s) - \beta(as) + 2\gamma P$, where $\Delta\kappa$ is the total phase mismatch, $\beta(x)$ is the propagation constant at either the pump (p), Stokes (s) or anti-Stokes (as) wavelengths, γ is the nonlinear coefficient of the fiber and P is the peak power of the pump pulse in the PCF. With this expression and the simulated modal propagation constants, it is possible to calculate the phase matching diagrams corresponding to the fast and slow axes of the fiber. These are shown in Fig. 5 as dashed and solid curves respectively. The vertical dotted line indicates the pump wavelength of 780 nm, and the intersection points with the phase matching curves predict the location of the Stokes and anti-Stokes wavelengths. The predicted sideband wavelengths were 642.5 nm and 992 nm for the slow axis, and 649.5 nm and 976 nm for the fast axis respectively. The inset figure shows the details of the difference in anti-Stokes wavelengths corresponding to both axes.

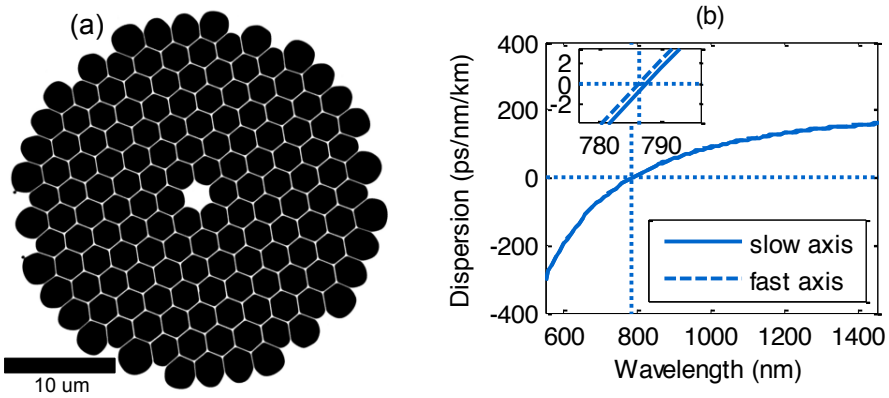

Fig. 4. (a) SEM image of the PCF, (b) dispersion profile of the fiber. The zero dispersion occurs at wavelength of 786.5 nm and 787.6 nm for fast and slow axis. The inset shows the details of the dispersion profile at zero dispersion wavelength for fast and slow axis.

The 780 nm light was then coupled into the PCF using suitable coupling optics (an aspheric lens with focal length of 4.6 mm was used to collimate the beam after the crystal module and another aspheric lens with focal length of 2.0 mm was used to focus the beam into the PCF). An 8.7 m length of this PCF was used in the experiment. This length was chosen by performing a cut-back on a longer length of the same PCF to determine the optimum power-length product for FWM. This prevented the onset of competing nonlinear spectral broadening while allowing strong FWM to occur. A half wave plate (HWP) was used to adjust the polarization state of the pump pulses coupled into the PCF, determining which axis of the fiber the light propagated on and thus the wavelengths of the Stokes and anti-Stokes output.

#223363 - $15.00 USD Received 17 Sep 2014; revised 21 Oct 2014; accepted 21 Oct 2014; published 20 Nov 2014

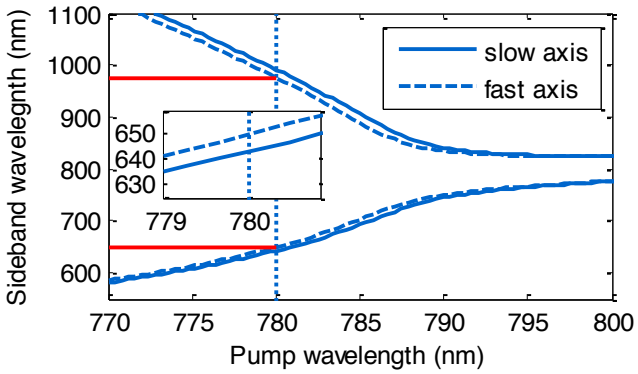

Fig. 5. Calculated phasematching diagrams for both fast and slow axis of the PCF. The inset shows the detail of the anti-stokes wavelengths for slow and fast axis.

Figure 6(a) shows the spectrum of the parametric wavelength conversion from the pump pulses spectrally centered at 780 nm to the Stokes wavelength centered at 938 nm and anti-Stokes wavelength centered at 668 nm. The anti-Stokes component was spectrally filtered and characterized. As shown in Fig. 6(b), the 3 dB linewidth of the anti-Stokes spectral output was 3.3 nm. The measurement was taken with 1.6 W pump power into PCF. The pulse duration (FWHM) of the anti-Stokes at 668 nm was 208 ps as shown in Fig. 6(c). This shortening of the pulse duration is expected for FWM due to the intensity dependent nature of the nonlinear conversion. The wings of the pulse have a lower intensity than the center and do not have the required intensity to undergo efficient FWM, resulting in a narrowing of the pulse in the time domain.

There are however differences between the predicted and observed parametric sideband positions. We attribute the deviation of the experimental results from the simulation results to two main reasons. Firstly, due to the high air filling fraction (> 90%) and corresponding very thin silica struts (~100 nm) in the cladding of the fiber structure, the dispersion curve and the phase matching diagram were very sensitive to the accuracy of the fiber SEM image and subsequent image processing for modal analysis. A different simulation was carried out with a minimal adjustment of the silica strut width, i.e. decrease of 1 pixel corresponding to thinning of struts by 18 nm. The zero dispersion wavelengths moved to 781 nm (slow axis) and 784 nm (fast axis). The sideband wavelengths changed to 670 nm and 930 nm for slow axis, and 703 nm and 875 nm for fast axis. The birefringence changed to 2.6×10^{-5} at 790 nm. Secondly, the simulation assumed uniformity of the refractive index profile along the axial direction of fiber. Slight structural variation in the actual fiber used would change the dispersion and birefringence properties as well as the phase matching conditions. In a similar fashion to the first point, the very high air-filling fraction of the PCF results in any slight change in structure causing a large change in the dispersive properties of the PCF.

#223363 - $15.00 USD Received 17 Sep 2014; revised 21 Oct 2014; accepted 21 Oct 2014; published 20 Nov 2014

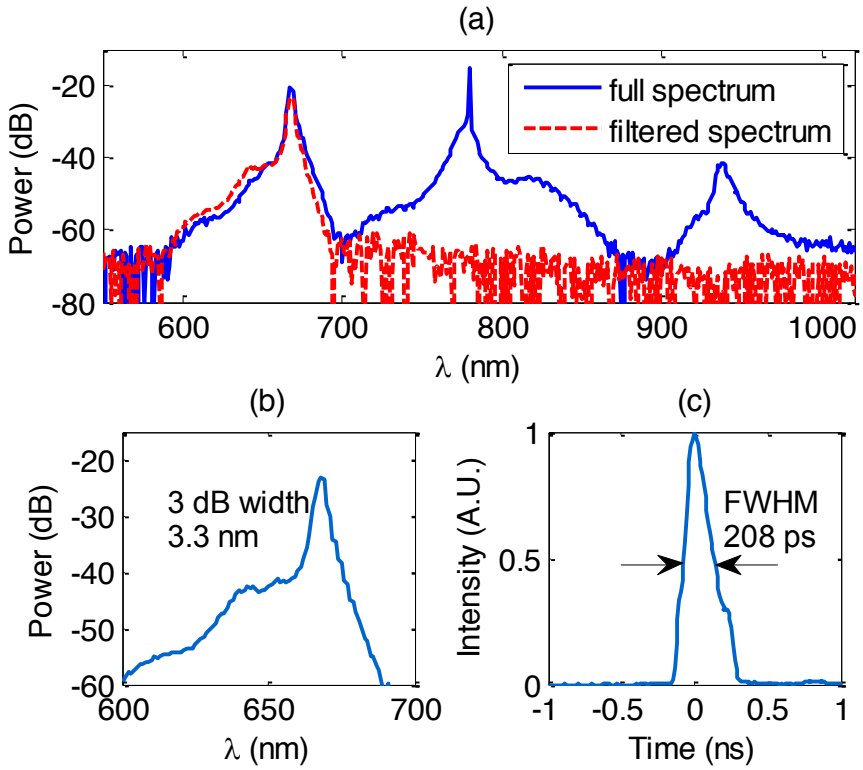

Fig. 6. (a) Spectra of the parametric wavelength conversion in the PCF showing pump and sidebands (b) spectrum of the anti-stokes output peaked at 668 nm, (c) pulse duration of anti-stokes measured by streak camera.

Figure 7 shows the average anti-Stokes output power for both axes of the PCF against the average pump power coupled into the PCF (taking the coupling efficiency of 66% into account). When the input power to the PCF was low (357 mW), the output power was measured to be 196 mW thus the insertion loss was 2.6 dB. At this low input power level, we assumed that the insertion loss was due to coupling loss and propagation loss only. The propagation loss was 0.77 dB, therefore the coupling loss was 1.83 dB, i.e. the coupling efficiency was 66%. We observed the generation of anti-Stokes light at 662 nm and 668 nm. Up to 105 mW was generated at 668 nm and 95 mW at 662 nm, with slope conversion efficiencies of 6.8% and 7.1% respectively.

#223363 - $15.00 USD Received 17 Sep 2014; revised 21 Oct 2014; accepted 21 Oct 2014; published 20 Nov 2014

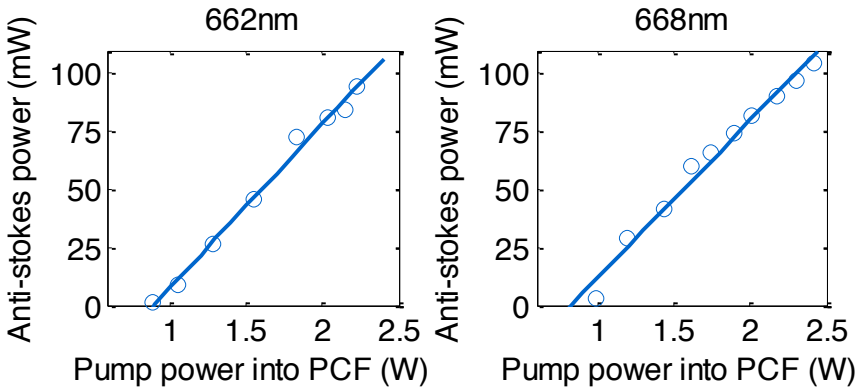

Fig. 7. Anti-stokes power of both axes as a function of pump power coupled into PCF.

3. Conclusion

In conclusion, we have demonstrated an all-fiber frequency-doubled erbium MOPFA system centered at 780 nm, with average power levels of 3.5 W. Using it as a pump source for FWM, we then demonstrated parametric wavelength conversion in a highly nonlinear PCF and generated anti-Stokes output at 668 nm and 662 nm, pulse durations of ~200 ps and average powers exceeding 95 mW. Such a source could find use in STED microscopy applications.

Acknowledgments

This work was supported in part by A*STAR Graduate Scholarship (Post-doctoral Fellowship, 2012-2014). EJRK acknowledges funding from the Royal Academy of Engineering. The authors would like to thank Dr Songnian Fu from Huazhong University of Science & Technology, China for helpful discussions.